Cell Reports

Report

Targeted Inactivation of *Bax* Reveals a Subtype-Specific Mechanism of Cajal-Retzius Neuron Death in the Postnatal Cerebral Cortex

Graphical Abstract

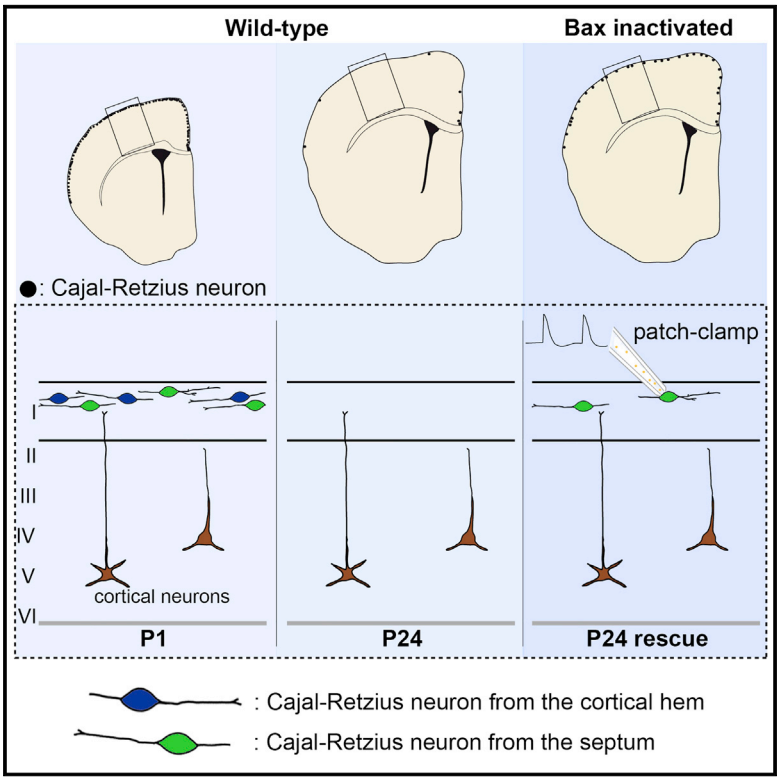

Highlights

- CR subtypes show differential cortical distribution at early postnatal ages
- Disappearance of CR subtypes is not synchronous in different cortical regions
- Bax-dependent and Bax-independent mechanisms drive death of CR subtypes
- Rescued CRs persist in an immature state in a mature environment

Authors

Fanny Ledonne, David Orduz, Judith Mercier, ..., Maria Cecilia Angulo, Alessandra Pierani, Eva Coppola

Correspondence

alessandra.pierani@ijm.fr (A.P.), eva.coppola@ijm.fr (E.C.)

In Brief

Ledonne et al. report that Cajal-Retzius neuron subtypes display unique distributions and dynamics of death in the postnatal mouse cortex. Conditional inactivation of the pro-apoptotic factor Bax reveals that different pathways control subtype death. CRs that are prevented from dying maintain immature electrophysiological properties in an adult environment.

Ledonne et al., 2016, Cell Reports *17*, 3133–3141
December 20, 2016
http://dx.doi.org/10.1016/j.celrep.2016.11.074

Cell Reports
Report

Targeted Inactivation of *Bax* Reveals a Subtype-Specific Mechanism of Cajal-Retzius Neuron Death in the Postnatal Cerebral Cortex

Fanny Ledonne,[1] David Orduz,[2,3] Judith Mercier,[1] Lisa Vigier,[1] Elisabeth A. Grove,[4] Fadel Tissir,[5] Maria Cecilia Angulo,[2,3] Alessandra Pierani,[1,6,*] and Eva Coppola[1,*]
[1]Institut Jacques Monod, CNRS UMR 7592, Université Paris Diderot, Sorbonne Paris Cité, 75205 Paris Cedex 13, France
[2]INSERM U1128, Paris, France
[3]Université Paris Descartes, Sorbonne Paris Cité, 75006 Paris, France
[4]Department of Neurobiology, University of Chicago, IL 60637, USA
[5]Université Catholique de Louvain, Institute of Neuroscience, 1200 Brussels, Belgium
[6]Lead Contact
*Correspondence: alessandra.pierani@ijm.fr (A.P.), eva.coppola@ijm.fr (E.C.)
http://dx.doi.org/10.1016/j.celrep.2016.11.074

SUMMARY

Cajal-Retzius cells (CRs), the first-born neurons in the developing cerebral cortex, coordinate crucial steps in the construction of functional circuits. CRs are thought to be transient, as they disappear during early postnatal life in both mice and humans, where their abnormal persistence is associated with pathological conditions. Embryonic CRs comprise at least three molecularly and functionally distinct subtypes: septum, ventral pallium/pallial-subpallial boundary (PSB), and hem. However, whether subtype-specific features exist postnatally and through which mechanisms they disappear remain unknown. We report that CR subtypes display unique distributions and dynamics of death in the postnatal mouse cortex. Surprisingly, although all CR subtypes undergo cell death, septum, but not hem, CRs die in a Bax-dependent manner. Bax-inactivated rescued septum-CRs maintain immature electrophysiological properties. These results underlie the existence of an exquisitely refined control of developmental cell death and provide a model to test the effect of maintaining immature circuits in the adult neocortex.

INTRODUCTION

The neocortex, an acquisition of the mammalian cerebral cortex, is organized in six-layers composed by both inhibitory and excitatory neurons. Lamination occurs through a sequential 'inside-out' order, whereby earlier-born neurons position in deeper layers and later-born migrate through older neurons to populate more superficial layers (Kwan et al., 2012). This process depends on the first generated neurons, Cajal-Retzius cells (CRs), which from the cortical surface, the future layer 1 (L1), orchestrate the radial migration of excitatory neurons through the extracellular matrix protein Reelin (Reln) (D'Arcangelo, 2005). Moreover, CRs play additional roles at multiple steps of cortical embryonic and postnatal development, positioning them as crucial players in the formation of functional neural circuits (Caronia-Brown and Grove, 2011; Kupferman et al., 2014).

Due to the common expression of Reln, CRs were long considered as a homogeneous population, but foregoing studies have underlined their heterogeneity, spreading from sites of origin, molecular signature, and possibly function. Indeed, CRs belong to distinct lineages generated from at least three progenitor domains at the border of the pallium: the cortical hem (CH) (Takiguchi-Hayashi et al., 2004; Yoshida et al., 2006), the ventral pallium (VP) at the pallial-subpallial boundary (PSB), and the pallial septum (Bielle et al., 2005). From these sources, CRs migrate tangentially to cover the entire surface of the cortex, and their different kinetics of migration underlie the specific CR subtype combination found in early cortical territories (Barber et al., 2015; Griveau et al., 2010). These studies also revealed that the elimination of septum-derived CRs or the altered distribution of CR subtypes lead to changes in the position and size of primary cortical areas (Griveau et al., 2010) or to the expansion of higher-order areas (Barber et al., 2015), respectively. This strongly supports the idea that CRs include multiple populations, each with specific characteristics and functions, during embryogenesis. However, in the postnatal brain, the behavior of CRs with different ontogenetic origins remains largely unknown.

Intriguingly, the vast majority of CRs disappear during early postnatal life, in mice as well as in primates, including humans (del Río et al., 1995; Derer and Derer, 1990; Meyer and Goffinet, 1998; Zecevic and Rakic, 2001). Several hypotheses were proposed to explain the loss of this entire population, such as their dilution in the growing cortex (Marín-Padilla, 1990) or their transfating into L1 Reln^{+} interneurons (Parnavelas and Edmunds, 1983). The most widely accepted theory to explain CRs loss is programmed cell death (PCD), based on the observation that some CRs present signs of degeneration of their axons and dendrites (Ma et al., 2014), picnotic nuclei (Derer and Derer, 1990), and cleaved-caspase-3 immunoreactivity (Anstötz et al., 2014; Chowdhury et al., 2010). It was proposed that CR apoptosis could be triggered by neural activity (Del Río et al.,

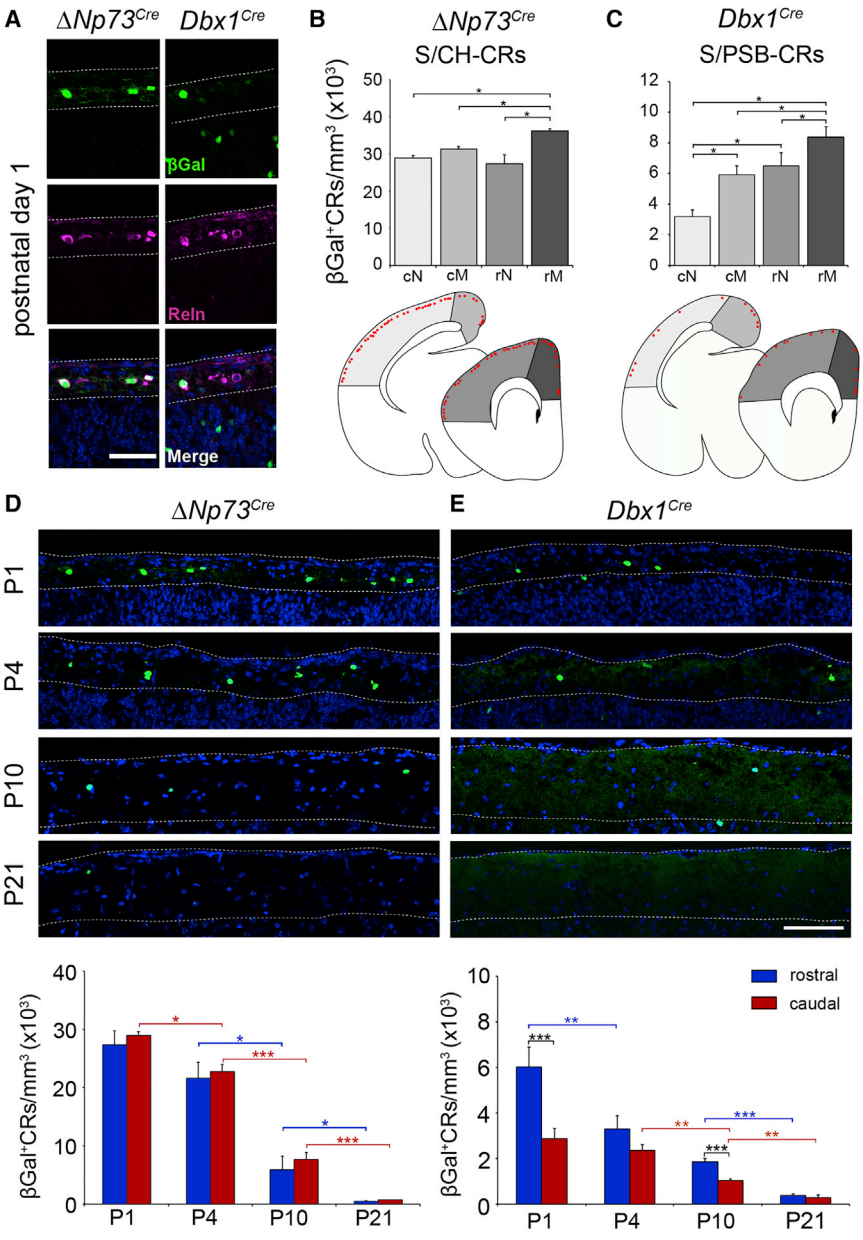

Figure 1. CR Subtype Distribution and Disappearance in the Postnatal Cortex

(A) Coronal section of P1 *ΔNp73^{Cre};Tau^{nlsLacZ}* and *Dbx1^{Cre};Tau^{nlsLacZ}* brains, immunostained for β-gal (green) and Reln (magenta). All reporter-positive neurons in layer 1 (L1) express Reln (S/CH-CRs, n = 75; S/PSB-CRs, n = 35).

(B and C) Countings and schemes of CRs density and distribution in *ΔNp73^{Cre};Tau^{nlsLacZ}* (B) and *Dbx1^{Cre};Tau^{nlsLacZ}* (C) brains at P1. Each red dot in the schemes represents one β-gal$^+$ neuron. cN, caudal neocortex; cM, caudo-medial cortex; rN, rostral neocortex; rM, rostro-medial cortex.

(D and E) β-gal immunostaining of coronal sections and cell density counts (β-gal$^+$ CRs/mm^3 [×10^3]) of the rostral (blue bars) and caudal (red bars) neocortex at P1, P4, P10, and P21 in *ΔNp73^{Cre};Tau^{nlsLacZ}* (D) and *Dbx1^{Cre};Tau^{nlsLacZ}* (E) mice.

Scale bars, 50 μm (A, D, and E). All values are expressed as mean ± SEM. n = 3 for each genotype; *p < 0.05, ***p < 0.001 Mann-Whitney test. Dashed lines correspond to the limit of L1. See also Figure S1.

RESULTS

Distribution and Disappearance of Cortical CR Subtypes at Postnatal Stages

To investigate whether CR subpopulations exhibited distinct features in the postnatal cortex, we used a permanent tracing strategy. We chose two Cre mouse lines, *ΔNp73^{Cre}*and *Dbx1^{Cre}*, which in combination with the *Tau^{GFPiresnlsLacZ}* reporter line allow one to reliably identify and follow either CRs derived from the septum and cortical hem (S/CH) (Tissir et al., 2009) or septum and PSB (S/PSB) (Bielle et al., 2005), respectively. We verified that all β-galactosidase-positive (β-gal$^+$) neurons in L1 also expressed Reln (Figure 1A) and none expressed GABA (Figure S1A), showing that both Cre lines specifically label CRs in L1 at postnatal ages, as already demonstrated during embryonic life.

We first compared the distribution of CRs in different cortical regions at postnatal day 1 (P1) in the two lines (Figures 1B and 1C). Overall, the density of S/CH CRs (labeled in the ΔNp73 lineage; Figure 1B) was at least four times higher than that of S/PSB CRs (labeled in the Dbx1 lineage; Figure 1C) depending on the cortical region, consistent with previous reports showing that the cortical hem is the main source of CRs throughout the neocortex (Gu et al., 2011; Tissir et al., 2009; Yoshida et al., 2006). The density of S/CH CRs was higher in the rostro-medial cortex than in any other region (Figure 1B), while that of S/PSB CRs was lower in the caudal neocortex and also higher in the rostro-medial cortex (Figure 1C). These results show that at

1996; Mienville et al., 1999), and a very recent study showed that excitatory GABAergic signaling mediated by the persistence of the chloride inward transporter NKCC1 is involved in CR death (Blanquie et al., 2016). However, due to the absence of specific markers to identify CR subtypes and follow them throughout life, whether cell death is the only mechanism involved in CR disappearance or whether trans-differentiation may contribute to this process is still a matter of debate.

In this report, we used genetic fate mapping to show that subtype-specific differences in the distribution and disappearance of CR subpopulations exist at the postnatal stages. We then showed, by conditionally eliminating the pro-apoptotic factor *Bax*, that different mechanisms drive the death of CR subtypes, with a Bax-dependent pathway for septum CRs, but not hem CRs.

P1, CR density and preferential distribution varies along the medio-lateral and rostro-caudal axes depending on the subtype.

We then investigated the dynamics of CR subtypes disappearance at three additional postnatal ages, namely P4, P10, and P21 (Figures 1D, 1E, S1B, and S1C). In the neocortex, the density of both S/CH-CRs and S/PSB-CRs was drastically reduced by P21 with only 2% and 6% of the perinatal pool left, respectively (Figures 1D and 1E). However, temporal and spatial differences in the dynamics of disappearance were observed between the two lines within the first 10 postnatal days. Indeed, the S/CH CR density drastically dropped at P10, with few differences along the rostro-caudal axis. In contrast, a strong reduction was detected for S/PSB CRs between P1 and P4 at rostral levels, while in the caudal neocortex, S/PSB CRs behaved like S/CH CRs. In the medial cortex, the global dynamics of disappearance followed that of the neocortex for each line except for a strong decrease in S/CH CR density observed at rostral levels at P4 (Figure S1C). This shows that overall, CRs start to decline within the first few postnatal days and that differences in the dynamics of disappearance between subtypes and within cortical territories exist, suggesting that both intrinsic and extrinsic mechanisms underlie distinct behaviors.

ΔNp73-Derived CRs Are Eliminated through a *Bax*-Dependent Mechanism

CR disappearance has been a controversial issue for several years. Using permanent genetic tracing in $\Delta Np73^{Cre}$; $Tau^{GFPiresnlsLacZ}$ P10 cortices, we found that all β-gal$^+$ cells resided exclusively in L1 (Figure S2A), where all coexpressed Reln, but not GABA, at postnatal stages (Figures 1A and S1A). This finding shows that trans-fating into Reln$^+$ GABAergic neurons does not occur in S/CH CRs. Furthermore, we estimated that the surface of the cerebral cortex grows ~2.2-fold between P4 and P24 (see Supplemental Experimental Procedures), indicating that dilution alone cannot account for the disappearance of 95% of CRs in the neocortex. We thus focused on the role of the pro-apoptotic factor *Bax*, one of the main players regulating apoptosis in different contexts, including the CNS (Buss et al., 2006; Southwell et al., 2012; White et al., 1998). We specifically inactivated Bax function in the cortical hem and septum using a mouse line harboring a floxed *Bax* allele and the $\Delta Np73^{Cre}$ line. We also introduced the reporter $Tau^{GFPiresPnlsLacZ}$ allele to identify CRs in which recombination had occurred and a full knockout allele for the *Bak* gene to analyze potential synergistic effects between these two pro-apoptotic factors, as suggested in other systems (Lindsten et al., 2000).

P24 brains of different genotypes were analyzed for the presence of β-gal$^+$ neurons in the neocortex (Figures 2A and 2B) and medial cortex (Figure S2B). Since all tested animals were carrying the reporter and the *Cre* alleles, we only indicate the state of *Bax* and *Bak* alleles. In the neocortex of double heterozygotes $Bax^{lox/+}$;$Bak^{+/-}$, we detected 723 ± 117 β-gal$^+$ CRs/mm^3, similarly to age-matched wild-types (609 ± 85 β-gal$^+$ CRs/mm^3) (Figure 2B). A more than 5-fold increase compared to controls was found in $Bax^{lox/lox}$;$Bak^{+/-}$ (4,256 ± 533 β-gal$^+$ CRs/mm^3), showing that the targeted elimination of *Bax* was sufficient to prevent death of a significant subpopulation of S/CH CRs. The concomitant absence of *Bak* did not provoke any additional rescue, indicating that the global inactivation of *Bak* does not affect S/CH CR survival. This is in agreement with previous observations that in differentiated neurons, Bak function does not provide any protection from apoptotic stimuli (Putcha et al., 2002). The CR identity of rescued β-gal$^+$ was confirmed using Reln and GABA immunostaining (Figure 2C). A similar rescue was also found in the medial cortex (Figure S2B) and at later ages (P54; data not shown), but not at P1 and P10, when we detected similar density in controls and mutants at the same age (Figure 2D). Very sparse β-gal$^+$ CRs were positive for activated caspase-3, a marker of the apoptotic process, at P10, when the highest number of CRs are lost (Figure 2E). Notably, both β-gal$^+$activated caspase-3$^+$ and β-gal$^+$activated caspase-3$^-$ cells were observed juxtaposed (Figure 2E), suggesting that synchronous death does not occur, even within the same territory. Overall, these data show that the rescue takes place after P10 and that ΔNp73 CR disappearance during early postnatal life occurs partly through cell-autonomous *Bax*-dependent apoptosis.

Rescued CRs Maintain Electrophysiological Properties of Immature Neurons

The proper molecular signature (Reln$^+$ and GABA$^-$) and the correct localization in L1 of rescued CRs (Figure 2C) do not ensure that they maintained a neuronal phenotype in the mature neocortex. We therefore performed patch-clamp recordings of rescued tdTomato$^+$ CRs in L1 at P24-28 using $BaxCKO^{\Delta Np73}$ mice backcrossed to the $ROSA26^{loxP\text{-}stop\text{-}loxP\text{-}Tomato}$ reporter mouse line. This time window corresponds to the age at which CRs have disappeared in the wild-type cortex (Figure 1). For comparison, we also recorded P8–P11 control CRs identified by the presence of tdTomato fluorescence triggered by *ΔNp73Cre*.

Since these cells are able to display spontaneous action potentials (APs) in acute slices from P5 (Mienville et al., 1999), we first recorded tdTomato$^+$ CRs in a cell-attached configuration (Figures 3A and 3B). Control and rescued CRs exhibited spontaneous neuronal discharges in 10 out of 22 cases whose frequency and coefficient of variation (CV) were not significantly different between the two postnatal age groups (Figures 3A and 3B; Table S1). Rescued CRs thus remain active on the network upon maturation of neuronal circuits. Next, we analyzed the basic properties and firing patterns of CRs (Figures 3C and 3D). At both postnatal ages, CRs were characterized by a high input resistance, a small capacitance, and a relatively depolarized resting potential as described for these cells before their disappearance in young mice (Table S1; reviewed in Kirischuk et al., 2014). Hyperpolarizing current pulses induced only a moderate sag in the two age groups as described in CRs after P6 (Zhou and Hablitz, 1996) (Figures 3C and 3D). As for control CRs recorded at P8–P11, some rescued CRs displayed multiple AP firing upon depolarizing current injections (Figures 3C and 3D), while others were unable to fire more than one AP. When a firing train was induced, the second spike exhibited an amplitude reduction and a pronounced duration increase (Table S1). These properties were characteristic of immature neurons (Kirischuk et al., 2014) as illustrated by the comparison of L1 interneurons recorded at P24–P28 in the same conditions

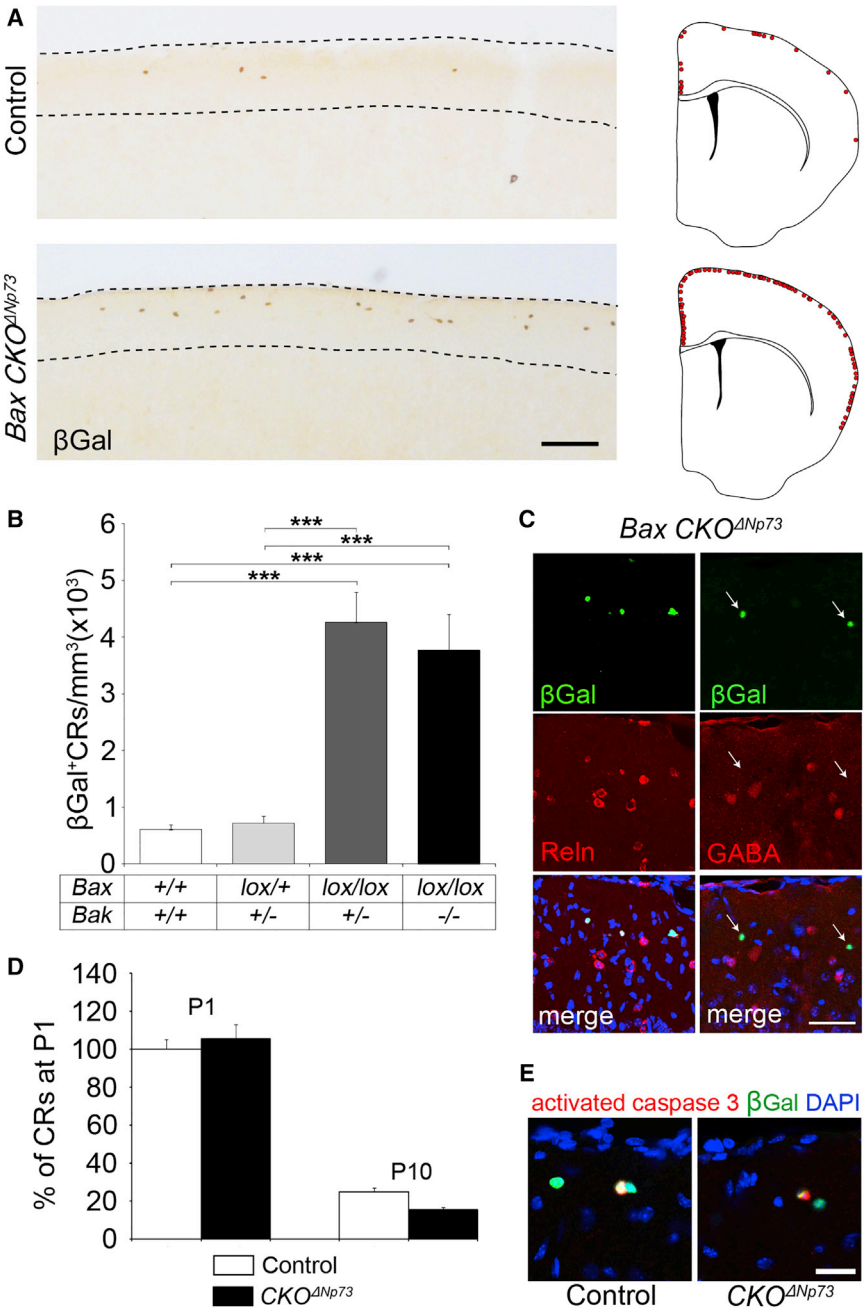

Figure 2. Invalidation of the Proapoptotic Gene *Bax* in the ΔNp73 Lineage Rescues CRs Death

(A) Coronal section of control ($\Delta Np73^{Cre}$) and $BaxCKO^{\Delta Np73}$ (all the samples are carrying the $Tau^{nlsLacZ}$ reporter) P24 neocortex immunostained for β-gal and schematic representations showing a whole section of control and $BaxCKO^{\Delta Np73}$ brains. Each dot corresponds to one β-gal$^+$ neuron. Dashed lines correspond to the limit of L1.

(B) Countings of β-gal$^+$ CR density (β-gal$^+$ CRs/mm^3) in the genetic backgrounds indicated on the x-axis: $Bax^{+/+};Bak^{+/+}$ (609 ± 85) and $Bax^{lox/+};Bak^{+/-}$ (723 ± 117), $Bax^{lox/lox}$; $Bak^{+/-}$ (4256 ± 533), $Bax^{lox/lox};Bak^{-/-}$ (3772 ± 630). Only the genotype of *Bax* and *Bak* alleles is indicated (all the samples are carrying the $Tau^{nlsLacZ}$ reporter and the $\Delta Np73^{Cre}$ genes).

(C) Immunofluorescence for β-gal (green) and Reln (n = 77) or GABA (n = 43) (red) on $BaxCKO^{\Delta Np73}$cortex at P24.

(D) Percentage of CRs at P1 and P10 in control and $BaxCKO^{\Delta Np73}$ with respect to the number in P1 controls (100%).

(E) Immunohistochemistry for βgal (green) and cleaved caspase-3 (red) at P10, counterstained for DAPI (blue), in control and $BaxCKO^{\Delta Np73}$ S/CH-CRs.

Scale bars, 100 μm (A), 50 μm (C), and 20 μm (E). All values are expressed as mean ± SEM. At least n = 3 for each genotype; ***p < 0.001. Mann-Whitney test. See also Figure S2.

Morphological reconstructions of recorded biocytin-loaded cells revealed that rescued CRs at P24 possessed the typical morphology of CRs (Figures 3G and S3E) (Anstötz et al., 2014), characterized by an ovoid or elongated somata and a bipolar morphology. We did not detect any difference in the volume occupied by the neuron, the total length of filaments, and the soma diameter between rescued CRs at P24 and control CRs (Table S1). However, the number of filament collaterals was reduced in rescued CRs at P24, which could explain their smaller membrane capacitance compared to control CRs (Figure S3). However, we observed some differences between control and rescued CRs. The first and second spike amplitudes as well as the hyperpolarizing slope of the first AP were reduced in rescued CRs compared to controls (Table S1). A longer latency between the AP peak and the after hyperpolarization was also observed in rescued CRs (Figure 3E; Table S1). Although the maximum firing frequency (F_{max}) was not statistically different between the two age groups (Table S1), rescued CRs exhibited less variable discharge frequencies and reached saturated discharge rates at lower current pulses (Figure 3F).

(Figures 3G–3J; Table S1). Interestingly, CRs reconstructed in mutant animals at P8–P11, although containing a mixture of CRs that within 1 week will die or whose death will be rescued by the Bax mutation (hereafter "rescued"), presented a homogeneous similar number of filament collaterals as control CRs at the same age (Figures 3G–3J). No differences in cell volume, soma diameter, and total filament length were detected between "rescued" cells at P8–P11, control cells at the same age, or rescued CRs at P24 (data not shown). This suggests that the reduction of filaments in P24 rescued CRs is due to aging of the neurons

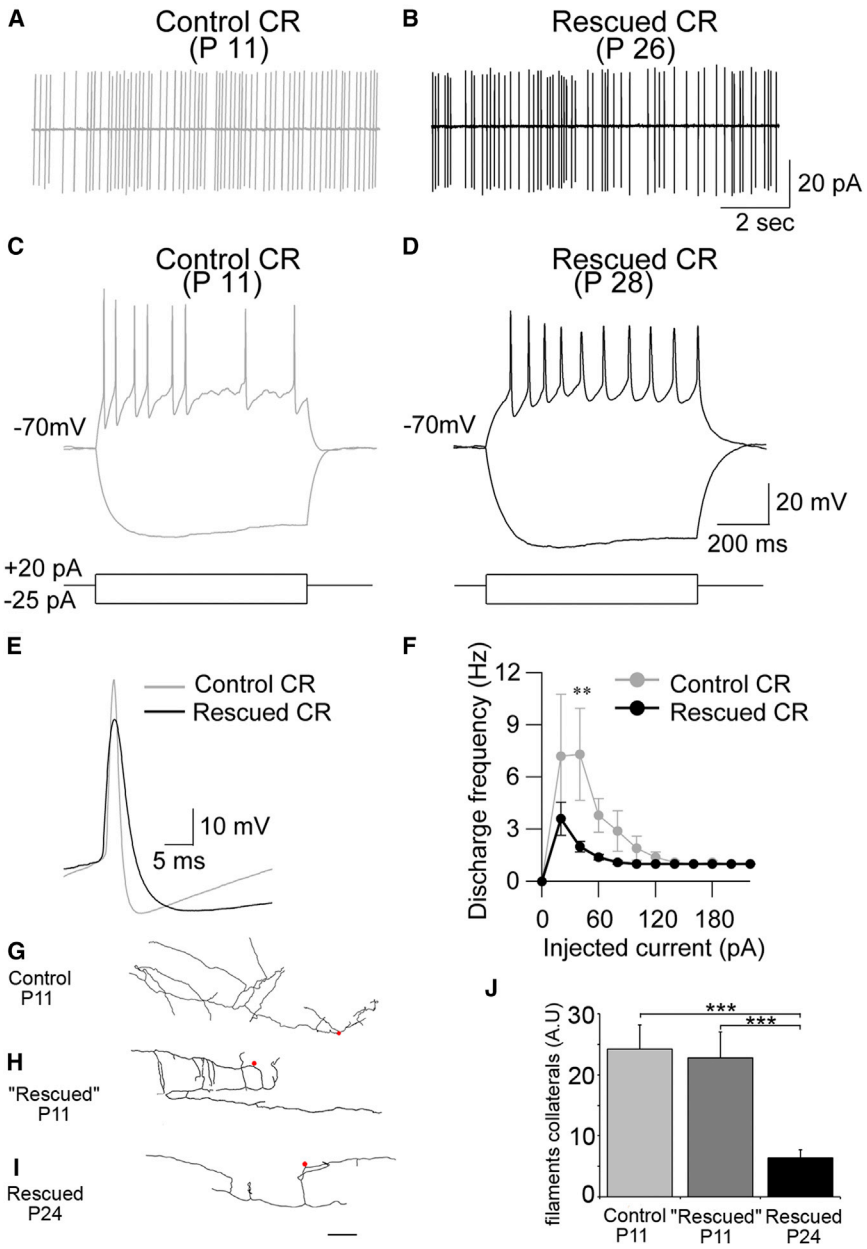

Figure 3. Spontaneous and Evoked APs in Control and Rescued *BaxCKO*$^{\Delta Np73}$ CRs

(A and B) Spontaneous spiking of a control (*ΔNp73*^{Cre};*ROSA*^{tdtomato}) (A) and a rescued CR (*BaxCKO*$^{\Delta Np73}$;*ROSA*^{tdtomato}) (B) during cell-attached recordings.

(C and D) Responses of a control (C) and a rescued CR (D) to hyperpolarized and depolarized current pulses during 800 ms at two different postnatal ages.

(E) Superimposed traces of the first AP recorded in (C) and (D).

(F) Plots of discharge frequencies as a function of injected current pulses for the two age groups (n = 10 for each group).

(G–I) Representative confocal reconstructions of biocytin-labeled P11 control (G), P11 "rescued" (H), and P24 rescued (I) CRs. Rescued CRs at P11 include both CRs prior to undergoing death and CRs that will survive. Soma is indicated in red.

(J) Change in filament collaterals among control P11, P11 rescued, and P24 rescued *BaxCKO*$^{\Delta Np73}$ CRs.

All values are expressed as mean ± SEM. Scale bars, 50 μm (G–I). **p < 0.01, Mann-Whitney test. See also Figure S3 and Table S1.

as proposed in Ma et al. (Ma et al., 2014) rather than a decreased initial growth.

Thus, despite some electrophysiological and morphological differences with control CRs, rescued CRs keep major CR morphological features and present electrophysiological properties of an immature neuron. These data show that rescued CRs maintain a neuronal phenotype and do not undergo firing maturation with postnatal development.

Wnt3A-Derived CH-CRs Die in a *Bax*-Independent Manner

In *BaxCKO*$^{\Delta Np73}$ mutants CR density in the neocortex was five times higher than in controls. However, even considering cortical growth between P1 and P24, it was not restored to values observed in P1 control brains, suggesting that the absence of *Bax* did not prevent the death of all *ΔNp73*^{Cre}-derived CRs (compare Figure 2B with Figures 1B and 1D). Since the *ΔNp73*^{Cre} should target *Bax* inactivation in distinct CR subtypes, we could not rule out whether the partial rescue observed in these mutants concerned CRs derived from the septum, CH, or both. To discriminate between these two CR subtypes, we inactivated Bax in CH-derived CRs using the *Wnt3a*^{Cre} mouse line, triggering Cre recombinase expression specifically in this subpopulation (Yoshida et al., 2006). First, we verified that at postnatal ages, all β-gal^{+} neurons expressed Reln, but not GABA (Figures 4A and S1A), in L1 of *Wnt3a*^{Cre};*Tau*^{GFPiresnlsLacZ} brains. We then analyzed the disappearance of labeled CH-CRs and observed a significant reduction between all postnatal ages at both rostral and caudal levels (Figure 4B), showing a fairly similar progression as in *ΔNp73*^{Cre};*Tau*^{GFPiresnlsLacZ} brains. Surprisingly, no differences in the number of neocortical CH-CRs were found when *Bax* was inactivated (*BaxCKO*^{Wnt3a}) compared to control brains at P24 (Figures 4C and 4D). We also found no increase in the number of β-gal^{+} cells upon elimination of *Bak* (Figure 4D). We thus tested whether a transient rescue of CH-CR death could have occurred at earlier postnatal ages and detected similar numbers of β-gal^{+} cells at P1 and P10 between *BaxCKO*^{Wnt3a} brains and controls (Figure 4E), despite the fact that very few

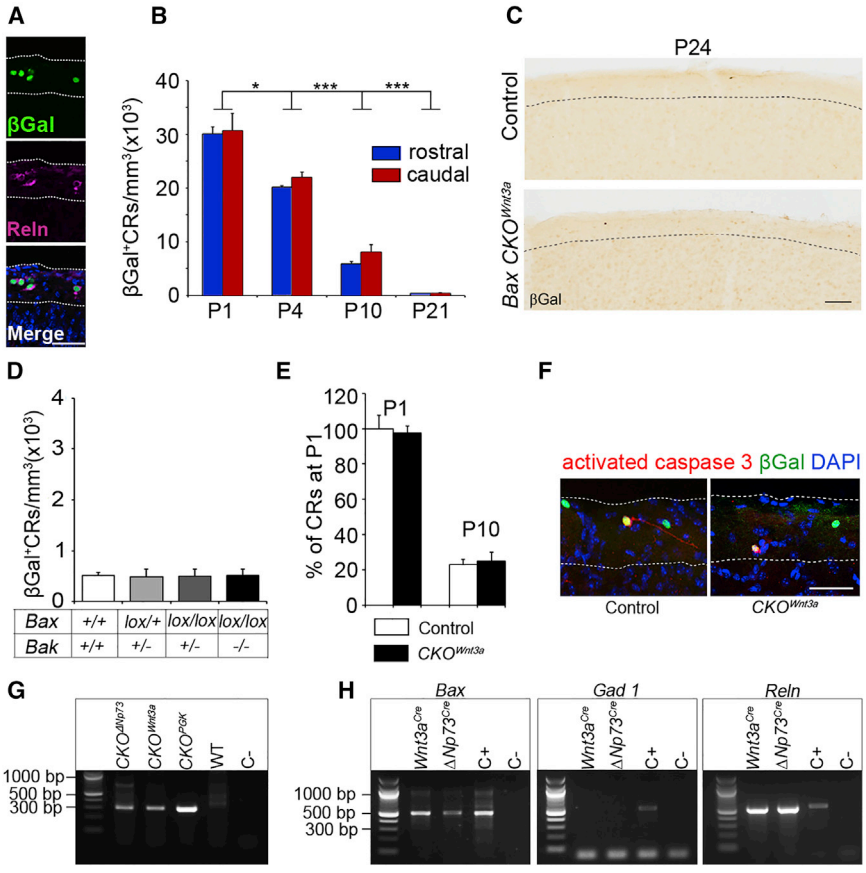

Figure 4. Invalidation of the Proapoptotic Gene *Bax* Does Not Prevent Death of CH-CRs

(A) Coronal section of P1 *Wnt3a*^{Cre};*Tau*^{nlsLacZ} brains, immunostained for β-gal (green) and Reln (magenta). All reporter-positive neurons in layer 1 (L1) express Reln (CH-CRs n = 173).

(B) β-gal immunostaining of coronal sections and cell density counts (β-gal$^+$ CRs/mm^3 [×10^3]) of the rostral (blue bars) and caudal (red bars) neocortex at P1, P4, P10, and P21 in *Wnt3a*^{Cre};*Tau*^{nlsLacZ} mice.

(C) Coronal section of control (*Wnt3a*^{Cre}) and *BaxCKO*^{Wnt3a} neocortex at P24 immunostained for β-gal.

(D) Quantification of β-gal$^+$CRs/mm^3 in the genetic backgrounds indicated on the x axis: *Bax*$^{+/+}$; *Bax*$^{+/+}$ (506 ± 66), *Bax*$^{lox/+}$;*Bak*$^{+/-}$ (484 ± 153), *Bax*$^{lox/lox}$;*Bax*$^{+/-}$ (502 ± 132) and *Bax*$^{lox/lox}$;Bak$^{-/-}$ (511 ± 120). Only the genotype of *Bax* and *Bak* alleles is indicated, all the samples are carrying the *Tau*^{nlsLacZ} reporter and the *Wnt3a*^{Cre} genes.

(E) Percentage of CRs at P1 and P10 in control and *BaxCKO*^{Wnt3a} with respect to the number in P1 controls (100%). All values are expressed as mean ± SEM.

(F) Immunohistochemistry for β-gal (green) and cleaved caspase-3 (red) at P10, counterstained for DAPI (blue), in control and *BaxCKO*^{Wnt3a} CH-CRs.

(G) CR-specific and ubiquitous recombination of the *Bax* allele in *BaxCKO*$^{\Delta Np73}$, *BaxCKO*^{Wnt3a}, and *BaxCKO*^{PGK} brains.

(H) RT-PCR for *Bax*, *Gad*1, and *Reln* in FACS-sorted tdTomato$^+$ CRs from P0 *ΔNp73*^{Cre};*ROSA*^{tdtomato} and *Wnt3a*^{Cre};*ROSA*^{tdtomato} brains. C+, control corresponding to tdTomato$^-$ cells. n = 3 for each genotype.

Scale bars represent 50 μm (A), 100 μm (C), and 50 μm (F). Dashed lines correspond to the limit of L1.

activated caspase-3$^+$ CH-CRs were detected in both conditions (Figure 4F). We verified that recombination of the Bax floxed allele occurred correctly in *BaxCKO*^{Wnt3a} mutants (Figure 4G). Furthermore, we showed that *Bax* mRNAs is expressed in fluorescence-activated cell sorting (FACS)-purified CH-CRs and S/CH-CRs from *Wnt3a*^{Cre};*ROSA26*^{tdTomato} and *ΔNp73*^{Cre};*ROSA26*^{tdTomato} cortices by RT-PCR. The molecular identity of sorted cells was controlled for *Reln* expression but absence of *Gad1* (Figure 4H). These data indicate that CH-CRs do not die in a Bax-dependent manner, even though at least some of them express Bax, and suggest that the partial rescue we observed in *BaxCKO*$^{\Delta Np73}$ mutants is due to survival of septum-derived CRs. Together, these results reveal that different pathways are involved in CR subtype death.

DISCUSSION

In this study, by combining genetic fate mapping, conditional gene inactivation, and electrophysiology, we show that the distribution, dynamics, and mechanisms of death differ among CR subtypes in the postnatal cortex.

CR subtypes were reported to display preferential repartition in the embryonic cortex with S-CRs populating the rostro-medial, CH-CRs the caudo-medial, and PSB-CRs the lateral pallium (Barber et al., 2015; Bielle et al., 2005; Griveau et al., 2010; Gu et al., 2011; Yoshida et al., 2006). In this study, we show that preferential distribution is maintained postnatally, with the density of ΔNp73-derived S/CH-CRs being higher in the rostro-medial cortex, while that of Dbx1-derived S/PSB-CRs is lower in the caudal neocortex. These distributions not only resemble very closely what was observed at early embryonic stages but also confirm time-lapse studies showing that the first streams of CRs are anchored from the earliest stages of corticogenesis to specific cortical territories and that their preferential distributions are established and, at least in part, maintained from these early stages (Barber et al., 2015). Although Dbx1-derived and non-derived CRs in the somatosensory cortex during the first postnatal week do not appear to display distinct electrophysiological properties (Sava et al., 2010), it is still possible that CR subtypes perform different functions in the early postnatal cortex. CRs receive GABAergic inputs from the subplate (Myakhar et al., 2011), a transient target of thalamic axons (Ghosh et al., 1990). Both subplate cells (SPs) and CRs disappear from the cerebral cortex by the end of the second postnatal week (Arias et al., 2002; Price et al., 1997), raising the intriguing possibility that microcircuits involving transient partners might shape area-specific cortical activity in mice.

We also show that subtype-specific dynamics of disappearance exist between Dbx1- and ΔNp73-derived CRs in both the neocortex and medial cortex, although they all reach a loss of

94%–97% by P21. S/PSB-CRs specifically displayed a faster loss during the first 4 postnatal days, and this in the neocortex at rostral levels. This is likely due to the faster death of PSB-CRs, which never express ΔNp73 (Bielle et al., 2005), the Δ isoform of P73 whose anti-apoptotic function was documented during development (Tissir et al., 2009). Furthermore, the delayed disappearance of S/CH-CRs was not detected in the medial cortex, showing that the different dynamics depend not only on the CR subtype but also on the cortical territories they reside in, reflecting that both intrinsic and extrinsic mechanisms underlie this diversity. Consistent with these observations, recent studies have shown that CRs remain detectable at least until 12 months of age in the hippocampus (Anstötz et al., 2016; Louvi et al., 2007), highlighting the role played by this environment in promoting survival or delaying CR death.

Although it is widely accepted that CRs are a transient population and some undergo apoptosis, whether dilution and/or trans-fating also played a role in CR disappearance postnatally is a matter of debate. Our results using permanent genetic tracing from all three sources of CR subtypes help solve this debate. First, we showed a loss of 94%–97% of all CR subtypes, in agreement with previous reports (Chowdhury et al., 2010; Ma et al., 2014) and that dilution cannot account for this reduction, since the cerebral cortex surface only increases at most by 2-fold between P4 and adulthood. Our results also allowed us to rule out CR trans-fating into Reln^{+} interneurons, a possibility that could not formally be excluded using reporters under the direct control of specific CR promoters, which might be inactivated if CRs changed fate.

By genetically targeting the inactivation of the pro-apoptotic factor Bax in specific CR subtype, we revealed that CR death can proceed through different mechanisms. Indeed, we showed that Bax exerted different effect on CR survival from the septum and the cortical hem and that CH-CRs, the main CR subtype population in the neocortex, were not rescued by Bax invalidation. We can exclude that rescued CRs observed in the *BaxCKO*$^{\Delta Np73}$ mutants result from remigration of CRs stored in the piriform cortex, as this reservoir is lost after E15.5 (de Frutos et al., 2016). It remains to be determined whether Bax controls PSB-CRs death, which we could not study, since the *Dbx1* and *Bax* genes are on the same chromosome.

Intriguingly, we and others (Anstötz et al., 2014; Chowdhury et al., 2010) have only been able to detect sparse labeling with activated caspase-3 in CRs. This is possibly due to the rapid turnover of activated caspase-3 and/or because synchronous death does not occur even within the same territory. Interestingly, Blanquie et al. (Blanquie et al., 2016) did not find changes in caspase-3 activation when CR survival was either diminished or augmented in an activity-dependent manner. Together, these data indicate that activated caspase-3 detection does not reflect CR death or rescue, arguing in favor of the possibility that activated caspase-3-dependent apoptosis is not the only mechanism by which CR loss takes place. Consistently, Anstötz et al. (2016) showed in the hippocampus that CR degeneration seems to be independent of caspase-3 activation. Our results show that PCD is exquisitely regulated in different neuronal populations. While all cortical interneurons (Southwell et al., 2012) appear to die in a Bax-dependent manner, we provide evidence that a Bax-independent pathway operates in CR developmental death. One possible mechanism could be excitotoxic cell death, which still occurs in the absence of Bax in cerebellar granule cells (Miller et al., 1997). It is tempting to propose that the multiple mechanisms controlling CR subtype elimination may serve a physiological function. Indeed, it has been shown that apoptotic cells have the unexpected capacity to stimulate either cell proliferation or further cell death (Pérez-Garijo et al., 2013). Specific death may represent the last signal delivered by CRs committed to die, which could produce different signals depending on the pathway driving their death and thus exert distinct effects on cortical function.

The CR-subtype-specific rescue obtained by targeted inactivation of Bax in the ΔNp73 lineage provides a mouse model where CRs persist in a normal cortical context. The comparison of different physiological characteristics between CRs in the second postnatal week and rescued CRs at later ages revealed that rescued CRs have unequivocally features of immature neurons and maintain most of their molecular, electrophysiological, and morphological properties. These cells thus remain in a developing state despite the maturation of other cortical neurons during postnatal development. The mouse model we have generated provides a tool to address the physiological meaning of CR disappearance in the postnatal animal. Notably, the abnormal persistence of CRs during postnatal life has been detected in pathological conditions, often those associated with epilepsy (Eriksson et al., 2001; Garbelli et al., 2001), thereby opening the intriguing possibility that the lack of their disappearance may be contributing to dysfunction of cortical circuits and altering early cortical networks. Our model will allow studying the effects of maintaining immature neurons in mature circuits and testing the role of CR PCD in cortical development and dysfunction.

EXPERIMENTAL PROCEDURES

Animals

A *Dbx1*^{IRESCre} (Bielle et al., 2005), *ΔNp73*^{CreIRESGFP} (Tissir et al., 2009), and *Wnt3a*^{Cre} (Yoshida et al., 2006), transgenic mice were kept in a C57BL/6J background. The *Bax*^{tm2Sjk};*Bak1*^{tm1Thsn}/J line (Takeuchi et al., 2005) harboring the floxed *Bax* allele and the *Bak* knockout allele was purchased from The Jackson Laboratory as mixed B6;129. *BaxCKO*$^{\Delta Np73}$ and *BaxCKO*^{Wnt3a} refer to *Bax* conditional knock out (CKO) using specific Cre mouse lines. All animals were handled in strict accordance with good animal practice as defined by the national animal welfare bodies, and all mouse work was approved by the Veterinary Services of Paris (authorization number: 75-1454) and by the Animal Experimentation Ethical Committee Buffon (CEEA-40) (reference: CEB-34-2012).

Brain Harvesting and Dissection

The day of birth was considered as P0. Animals were anesthetized by intraperitoneal injection of 0.5 μL/g pentobarbital sodique (CEVA), intracardially perfused with 4% paraformaldehyde (PFA) in 0.1 M PBS (pH 7.4) and post-fixed overnight in 4% PFA at 4°C. Brains were cryoprotected overnight in 20% sucrose and embedded in O.C.T. compound (Tissue Tek). Embedded brains were sectioned on a cryostat at 12 μm thickness between P1 and P10 and 50 μm thickness for mice older than P10. Immunostaining was performed as previously described (Bielle et al., 2005; Griveau et al., 2010).

Acute Slice Preparation and Electrophysiology

Acute coronal slices (300 μm) of the neocortex were obtained from control mice at P9–P11 and *BaxCKO*$^{\Delta Np73}$ mutants at P24–P28. Excitation light to visualize the tdTomato fluorescent protein was provided by a green Optoled

Light Source (Cairn Research), and images were collected with an iXon+ 14-bit digital camera (Andor Technology), as previously described (Orduz et al., 2015).

Statistical Analysis

All values are expressed as mean ± SEM. For pairwise comparison, statistical significance was determined using the nonparametric Mann-Whitney test. Multiple group comparisons were done using a two-way ANOVA and Bonferroni post-tests.

Detailed protocols are included in Supplemental Experimental Procedures.

SUPPLEMENTAL INFORMATION

Supplemental Information includes Supplemental Experimental Procedures, three figures, and one table and can be found with this article online at http://dx.doi.org/10.1016/j.celrep.2016.11.074.

AUTHOR CONTRIBUTIONS

F.L., E.C., and D.O. designed and performed the experiments, J.M. analyzed the *Wnt3a*^{Cre};*Bax*CKO phenotype, E.A.G. and F.T. provided the *Wnt3a*^{Cre} and *ΔNp73*^{Cre}mouse line, and L.V. helped with animal maintenance. A.P., E.C., and M.C.A. supervised the project and analyzed data. F.L., D.O., M.C.A., E.C., and A.P. wrote the manuscript.

ACKNOWLEDGMENTS

We acknowledge the Imago Seine facility, a member of the France BioImaging infrastructure supported by the French National Research Agency (ANR-10-INSB-04, "Investments for the future"), for help with confocal microscopy; E. Franck for FACS; Animalliance and A. Dutriaux for animal care and maintenance; and J. Youale for contributing analyzing *Wnt3a*^{Cre} lineage. F.L. was the recipient of fellowships from Region Ile de France DIM Cerveau et Pensée and FFRE (Fondation française pour la recherche sur l'épilépsie). A.P. and M.C.A are CNRS (Centre National de la Recherche Scientifique) Investigators and member teams of the École des Neurosciences de Paris Ile-de-France (ENP). E.C. is a University Paris Diderot lecturer. This work was supported by the Agence Nationale de la Recherche(grants ANR-2011-BSV4-023-01 and ANR-15-CE16-0003-01), the FRM (grant ≪Equipe FRM DEQ20130326521≫), and Fédération pour la Recherche sur le Cerveau (FRC) (A.P.). This work was also supported by grant ANR-15-CE16-0003 and Idex Université Sorbonne Paris Cité (A.P. and M.C.A.) and by FRM grant (≪Equipe FRM DEQ20150331681≫) (M.C.A.).

Received: March 17, 2016
Revised: September 26, 2016
Accepted: November 23, 2016
Published: December 20, 2016

REFERENCES

Anstötz, M., Cosgrove, K.E., Hack, I., Mugnaini, E., Maccaferri, G., and Lübke, J.H. (2014). Morphology, input-output relations and synaptic connectivity of Cajal-Retzius cells in layer 1 of the developing neocortex of CXCR4-EGFP mice. Brain Struct. Funct. *219*, 2119–2139.

Anstötz, M., Huang, H., Marchionni, I., Haumann, I., Maccaferri, G., and Lübke, J.H. (2016). Developmental profile, morphology, and synaptic connectivity of Cajal-Retzius cells in the postnatal mouse hippocampus. Cereb. Cortex *26*, 855–872.

Arias, M.S., Baratta, J., Yu, J., and Robertson, R.T. (2002). Absence of selectivity in the loss of neurons from the developing cortical subplate of the rat. Brain Res. Dev. Brain Res. *139*, 331–335.

Barber, M., Arai, Y., Morishita, Y., Vigier, L., Causeret, F., Borello, U., Ledonne, F., Coppola, E., Contremoulins, V., Pfrieger, F.W., et al. (2015). Migration speed of Cajal-Retzius cells modulated by vesicular trafficking controls the size of higher-order cortical areas. Curr. Biol. *25*, 2466–2478.

Bielle, F., Griveau, A., Narboux-Nême, N., Vigneau, S., Sigrist, M., Arber, S., Wassef, M., and Pierani, A. (2005). Multiple origins of Cajal-Retzius cells at the borders of the developing pallium. Nat. Neurosci. *8*, 1002–1012.

Blanquie, O., Liebmann, L., Hübner, C.A., Luhmann, H.J., and Sinning, A. (2016). NKCC1-mediated GABAergic signaling promotes postnatal cell death in neocortical Cajal-Retzius cells. Cereb. Cortex, Published online January 26, 2016. http://dx.doi.org/10.1093/cercor/bhw004.

Buss, R.R., Sun, W., and Oppenheim, R.W. (2006). Adaptive roles of programmed cell death during nervous system development. Annu. Rev. Neurosci. *29*, 1–35.

Caronia-Brown, G., and Grove, E.A. (2011). Timing of cortical interneuron migration is influenced by the cortical hem. Cereb. Cortex *21*, 748–755.

Chowdhury, T.G., Jimenez, J.C., Bomar, J.M., Cruz-Martin, A., Cantle, J.P., and Portera-Cailliau, C. (2010). Fate of cajal-retzius neurons in the postnatal mouse neocortex. Front. Neuroanat. *4*, 10.

D'Arcangelo, G. (2005). The reeler mouse: anatomy of a mutant. Int. Rev. Neurobiol. *71*, 383–417.

de Frutos, C.A., Bouvier, G., Arai, Y., Thion, M.S., Lokmane, L., Keita, M., Garcia-Dominguez, M., Charnay, P., Hirata, T., Riethmacher, D., et al. (2016). Reallocation of olfactory Cajal-Retzius cells shapes neocortex architecture. Neuron *92*, 435–448.

del Río, J.A., Martínez, A., Fonseca, M., Auladell, C., and Soriano, E. (1995). Glutamate-like immunoreactivity and fate of Cajal-Retzius cells in the murine cortex as identified with calretinin antibody. Cereb. Cortex *5*, 13–21.

Del Río, J.A., Heimrich, B., Supèr, H., Borrell, V., Frotscher, M., and Soriano, E. (1996). Differential survival of Cajal-Retzius cells in organotypic cultures of hippocampus and neocortex. J. Neurosci. *16*, 6896–6907.

Derer, P., and Derer, M. (1990). Cajal-Retzius cell ontogenesis and death in mouse brain visualized with horseradish peroxidase and electron microscopy. Neuroscience *36*, 839–856.

Eriksson, S.H., Thom, M., Heffernan, J., Lin, W.R., Harding, B.N., Squier, M.V., and Sisodiya, S.M. (2001). Persistent reelin-expressing Cajal-Retzius cells in polymicrogyria. Brain *124*, 1350–1361.

Garbelli, R., Frassoni, C., Ferrario, A., Tassi, L., Bramerio, M., and Spreafico, R. (2001). Cajal-Retzius cell density as marker of type of focal cortical dysplasia. Neuroreport *12*, 2767–2771.

Ghosh, A., Antonini, A., McConnell, S.K., and Shatz, C.J. (1990). Requirement for subplate neurons in the formation of thalamocortical connections. Nature *347*, 179–181.

Griveau, A., Borello, U., Causeret, F., Tissir, F., Boggetto, N., Karaz, S., and Pierani, A. (2010). A novel role for Dbx1-derived Cajal-Retzius cells in early regionalization of the cerebral cortical neuroepithelium. PLoS Biol. *8*, e1000440.

Gu, X., Liu, B., Wu, X., Yan, Y., Zhang, Y., Wei, Y., Pleasure, S.J., and Zhao, C. (2011). Inducible genetic lineage tracing of cortical hem derived Cajal-Retzius cells reveals novel properties. PLoS ONE *6*, e28653.

Kirischuk, S., Luhmann, H.J., and Kilb, W. (2014). Cajal-Retzius cells: update on structural and functional properties of these mystic neurons that bridged the 20th century. Neuroscience *275*, 33–46.

Kupferman, J.V., Basu, J., Russo, M.J., Guevarra, J., Cheung, S.K., and Siegelbaum, S.A. (2014). Reelin signaling specifies the molecular identity of the pyramidal neuron distal dendritic compartment. Cell *158*, 1335–1347.

Kwan, K.Y., Sestan, N., and Anton, E.S. (2012). Transcriptional co-regulation of neuronal migration and laminar identity in the neocortex. Development *139*, 1535–1546.

Lindsten, T., Ross, A.J., King, A., Zong, W.X., Rathmell, J.C., Shiels, H.A., Ulrich, E., Waymire, K.G., Mahar, P., Frauwirth, K., et al. (2000). The combined functions of proapoptotic Bcl-2 family members bak and bax are essential for normal development of multiple tissues. Mol. Cell *6*, 1389–1399.

Louvi, A., Yoshida, M., and Grove, E.A. (2007). The derivatives of the Wnt3a lineage in the central nervous system. J. Comp. Neurol. *504*, 550–569.

Ma, J., Yao, X.H., Fu, Y., and Yu, Y.C. (2014). Development of layer 1 neurons in the mouse neocortex. Cereb. Cortex *24*, 2604–2618.

Marín-Padilla, M. (1990). Three-dimensional structural organization of layer I of the human cerebral cortex: a Golgi study. J. Comp. Neurol. *299*, 89–105.

Meyer, G., and Goffinet, A.M. (1998). Prenatal development of reelin-immunoreactive neurons in the human neocortex. J. Comp. Neurol. *397*, 29–40.

Mienville, J.M., Maric, I., Maric, D., and Clay, J.R. (1999). Loss of IA expression and increased excitability in postnatal rat Cajal-Retzius cells. J. Neurophysiol. *82*, 1303–1310.

Miller, T.M., Moulder, K.L., Knudson, C.M., Creedon, D.J., Deshmukh, M., Korsmeyer, S.J., and Johnson, E.M., Jr. (1997). Bax deletion further orders the cell death pathway in cerebellar granule cells and suggests a caspase-independent pathway to cell death. J. Cell Biol. *139*, 205–217.

Myakhar, O., Unichenko, P., and Kirischuk, S. (2011). GABAergic projections from the subplate to Cajal-Retzius cells in the neocortex. Neuroreport *22*, 525–529.

Orduz, D., Maldonado, P.P., Balia, M., Velez-Fort, M., de Sars, V., Yanagawa, Y., Emiliani, V., and Angulo, M.C. (2015). Interneurons and oligodendrocyte progenitors form a structured synaptic network in the developing neocortex. Elife *4*. http://dx.doi.org/10.7554/eLife.06953.

Parnavelas, J.G., and Edmunds, S.M. (1983). Further evidence that Retzius-Cajal cells transform to nonpyramidal neurons in the developing rat visual cortex. J. Neurocytol. *12*, 863–871.

Pérez-Garijo, A., Fuchs, Y., and Steller, H. (2013). Apoptotic cells can induce non-autonomous apoptosis through the TNF pathway. eLife *2*, e01004.

Price, D.J., Aslam, S., Tasker, L., and Gillies, K. (1997). Fates of the earliest generated cells in the developing murine neocortex. J. Comp. Neurol. *377*, 414–422.

Putcha, G.V., Harris, C.A., Moulder, K.L., Easton, R.M., Thompson, C.B., and Johnson, E.M., Jr. (2002). Intrinsic and extrinsic pathway signaling during neuronal apoptosis: lessons from the analysis of mutant mice. J. Cell Biol. *157*, 441–453.

Sava, B.A., Dávid, C.S., Teissier, A., Pierani, A., Staiger, J.F., Luhmann, H.J., and Kilb, W. (2010). Electrophysiological and morphological properties of Cajal-Retzius cells with different ontogenetic origins. Neuroscience *167*, 724–734.

Southwell, D.G., Paredes, M.F., Galvao, R.P., Jones, D.L., Froemke, R.C., Sebe, J.Y., Alfaro-Cervello, C., Tang, Y., Garcia-Verdugo, J.M., Rubenstein, J.L., et al. (2012). Intrinsically determined cell death of developing cortical interneurons. Nature *491*, 109–113.

Takeuchi, O., Fisher, J., Suh, H., Harada, H., Malynn, B.A., and Korsmeyer, S.J. (2005). Essential role of BAX,BAX in B cell homeostasis and prevention of autoimmune disease. Proc. Natl. Acad. Sci. USA *102*, 11272–11277.

Takiguchi-Hayashi, K., Sekiguchi, M., Ashigaki, S., Takamatsu, M., Hasegawa, H., Suzuki-Migishima, R., Yokoyama, M., Nakanishi, S., and Tanabe, Y. (2004). Generation of reelin-positive marginal zone cells from the caudomedial wall of telencephalic vesicles. J. Neurosci. *24*, 2286–2295.

Tissir, F., Ravni, A., Achouri, Y., Riethmacher, D., Meyer, G., and Goffinet, A.M. (2009). DeltaNp73 regulates neuronal survival in vivo. Proc. Natl. Acad. Sci. USA *106*, 16871–16876.

White, F.A., Keller-Peck, C.R., Knudson, C.M., Korsmeyer, S.J., and Snider, W.D. (1998). Widespread elimination of naturally occurring neuronal death in Bax-deficient mice. J. Neurosci. *18*, 1428–1439.

Yoshida, M., Assimacopoulos, S., Jones, K.R., and Grove, E.A. (2006). Massive loss of Cajal-Retzius cells does not disrupt neocortical layer order. Development *133*, 537–545.

Zecevic, N., and Rakic, P. (2001). Development of layer I neurons in the primate cerebral cortex. J. Neurosci. *21*, 5607–5619.

Zhou, F.M., and Hablitz, J.J. (1996). Postnatal development of membrane properties of layer I neurons in rat neocortex. J. Neurosci. *16*, 1131–1139.